DOI:10.1021/jf903170b

JOURNAL OF AGRICULTURAL AND FOOD CHEMISTRY
ARTICLE

Phytoglycogen Octenyl Succinate, an Amphiphilic Carbohydrate Nanoparticle, and ε-Polylysine To Improve Lipid Oxidative Stability of Emulsions

Siqi L Scheffler, Xue Wang, Lei Huang, Fernanda San-Martin Gonzalez, and Yuan Yao*

The Department of Food Science, Purdue University, 745 Agriculture Mall Drive, West Lafayette, Indiana 47907-1160

Phytoglycogen octenyl succinate (PG-OS) and ε-polylysine (EPL) were used to form oil-in-water emulsions with enhanced lipid oxidative stability. PG-OS is an amphiphilic carbohydrate nanoparticle prepared using octenyl succinate (OS) substitution of phytoglycogen (PG). PG-OS had a dispersed molecular density nearly 20 times that of waxy corn starch octenyl succinate (WCS-OS). Fish oil-in-water emulsions were prepared using PG-OS, WCS-OS, and Tween 20, stored at 55 °C for 6 days, and monitored for the accumulation of hydroperoxide and thiobarbituric acid reactive substances (TBARS). The result indicated that PG-OS may lead to high lipid oxidative stability, and that the addition of EPL may further improve the oxidative stability of emulsions. To address the interaction between PG-OS and EPL, zeta-potential was determined for various systems. The results indicated a possible formation of an interfacial complex layer comprising both PG-OS and EPL. This complex layer may provide both physical and electrostatic barriers against pro-oxidative compounds.

KEYWORDS: Phytoglycogen octenyl succinate; ε-polylysine; emulsion; oxidative stability

INTRODUCTION

Phytoglycogen is a starchlike α-D-glucan present in plants. Different from starch, phytoglycogen does not show the semicrystalline structure of starch and is water-dispersible due to its high branch density. The largest source of phytoglycogen is the kernel of the maize mutant *sugary-1* (*su1*), a primary genotype of commercial sweet corn. The *su1* mutation leads to the deficiency of SU1, an isoamylase-type starch debranching enzyme (DBE) (*1*). In the biosynthesis of starch, starch synthase, starch branching enzyme, and DBE work coordinately to produce starch granules (*2*). The primary role of DBE is to trim abnormal branches that inhibit the formation of starch crystals and granules (*3*, *4*). In the absence of DBE, the highly branched phytoglycogen is formed to replace starch.

Transmission electron microscope (TEM) and cryo-TEM showed that phytoglycogen ranges from 30 to 100 nm in particle size and exhibits a spherical shape (*5*). Our recent works using TEM and cryo-SEM indicated similar particle size and shape for most phytoglycogen particles (data not shown). The highly branched structure of phytoglycogen results in its unusually high molecular density in dispersion. In rice, the dispersed molecular density of PG is over 10 times that of starch (*6*). As depicted in **Figure 1**, each phytoglycogen nanoparticle may contain thousands of glucan chains forming the highly branched and packed structure. While not fully understood, it is likely that the particles grow from the nonreducing ends of glucan chains at the surface by periodic branching and elongation of chains. As shown in **Figure 1**, for a phytoglycogen molecule, there is no long chain that connects individual clusters as for amylopectin (*7*, *8*), which leads to the fundamental structural difference between phytoglycogen and amylopectin.

The preparation of starch octenyl succinate dated back to 1953 by Caldwell and Wurzburg to create effective emulsifiers using starch (*9*). Recently, a number of research studies have been published on the characterization and optimization of starch octenyl succinate (*10*−*13*). In emulsion, starch octenyl succinate offers both steric hindrance and electrostatic repulsion among oil droplets, thus leading to high stability of emulsions. It has shown superior functionality compared with gum arabic for encapsulating flavors and fish oil, especially for improving oxidation stability (*14*).

ε-Polylysine (EPL) is a cationic, naturally occurring homopolyamide of L-lysine produced by *Streptomyces albulus* (*15*). In EPL molecules, the amide linkages are formed between the ε-amino and α-carboxyl groups (**Figure 2**). EPL is water-soluble, biodegradable, edible, and nontoxic, and has been used in a variety of applications such as food preservatives, emulsifying agent, dietary agent, biodegradable fibers, highly water absorbable hydrogels, and other functional agents (*15*). However, there is no report of using EPL as an antioxidant in either emulsion or nonemulsion systems.

Reducing lipid oxidation is essential for improving the stability of oil-in-water emulsions widely used in the food, nutraceutical, drug, personal care, and other industries. A number of strategies have been developed to reduce the rate of lipid autoxidation (*16*−*18*).

*Corresponding author. Phone: (765) 494-6317. Fax: (765) 494-7953. E-mail: yao1@purdue.edu.

 Published on Web 11/23/2009

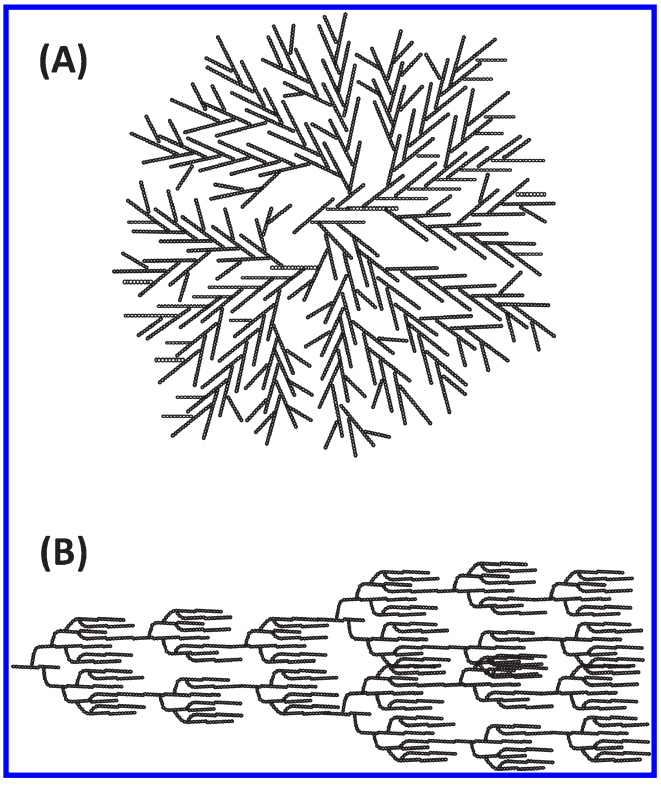

Figure 1. Two-dimensional schematic of a phytoglycogen nanoparticle (**A**) and a segment of amylopectin (**B**).

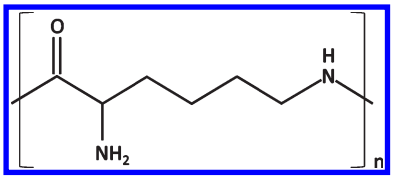

Figure 2. Structure of ε-polylysine.

These include (1) reducing free radicals by using radical scavenging antioxidants, (2) reducing oxidation catalysts, such as transition metal ions and singlet oxygen, and (3) inactivating oxidation intermediate, such as hydroperoxide (*17*). In oil-in-water emulsions, lipid oxidation mostly occurs at the interface and specific approaches can be designed to control the oxidation process. In addition to using radical scavenging antioxidants and chelators, interfacial properties are essential to the control of intermediate and final oxidation products (*18*). For example, forming a positively charged and/or thick interfacial layer may reduce the interactions of hydroperoxide and pro-oxidants such as metal ions and oxygen (*19*−*22*). Further, it was considered that the density of the interfacial layer affects the permeation of pro-oxidative compounds (*23*).

The purpose of this study was to determine the effect of amphiphilic carbohydrate nanoparticles on improving oxidative stability of emulsions. Phytoglycogen octenyl succinate was created and used as the model carbohydrate nanoparticle. It was further expected that oxidative stability could be improved by using ε-polylysine due to its interfacial repulsion effect against metal ions. It was anticipated that a combined use of both carbohydrate nanoparticles and ε-polylysine could form a complex layer at the oil−water interface and thus provide both physical and electrostatic barriers against pro-oxidative compounds. This strategy can be applied to a broad variety of areas to reduce lipid oxidation for improving lipid-containing systems.

MATERIALS AND METHODS

Materials. Waxy corn starch (WCS) was a gift from National Starch Food Innovation (Bridgewater, NJ). Sweet corn Silver Queen (a *sugary* hybrid) was purchased from Burpee Co. (Warminster, PA). 1-Octenyl succinate anhydride (OSA) was a gift from Dixie Chemical Co. (Houston, TX). Fish oil from menhaden and Tween 20 were purchased from Sigma-Aldrich (St. Louis, MO). ε-Polylysine (25.8% w/w in water) was obtained from Purac America (Lincolnshire, IL).

Methods. *Extraction of Phytoglycogen.* Sweet corn kernels were ground into grits and then mixed with 4 to 6 weights of deionized water. The suspension was homogenized using a high-speed blender (Waring Laboratory, Torrington, CT) and then centrifuged at 5500*g* for 20 min. The supernatant was collected whereas the solid was further extracted twice using deionized water. Thereafter, the supernatant at each batch was combined and passed through a 270-mesh sieve. The liquid was then added to 3 volumes of ethanol to precipitate the polysaccharide. After centrifugation and decanting the supernatant, the precipitate was further dispersed using 3 volumes of ethanol and centrifuged to dehydrate. The suspension after the last ethanol addition was filtered to remove excess liquid. The solid material was placed in a fume hood to remove residual ethanol. The powder collected was the phytoglycogen material used for further treatments.

Substitution Using Octenyl Succinic Anhydride. To the suspension of waxy corn starch (20% w/w) and dispersion of phytoglycogen (20%, w/w), 1-octenyl succinate anhydride was gradually added in 2 h at the levels of 3 and 9% based on the dry weight of glucans. The pH was maintained between 8.5 and 9.0 using 2% NaOH. The reaction was conducted at room temperature (22 °C) and terminated after 24 h by reducing the pH to 6.5 using 2% HCl. To collect substituted glucans, three volumes of ethanol were added to the reaction mixture. The precipitated materials were collected and further dehydrated using 3 cycles of ethanol suspension−centrifugation. The solid collected after filtration was placed in a fume hood to remove residual ethanol to prepare dry powder of phytoglycogen octenyl succinate.

Degree of substitution (DS) of phytoglycogen octenyl succinate and waxy corn starch octenyl succinate was determined using a method from the Joint FAO/WHO Expert Committee on Food Additives (*24*) with modifications. The glucan sample (0.5 g) was acidified with 3 mL of HCl (2.5 M) for 30 min. To each mixture, 10 mL of 90% isopropanol (v/v) was added, followed by centrifugation at 3000*g* for 10 min and supernatant decanting. To the precipitate, an additional 10 mL of 90% isopropanol was added to resuspend the glucan solid, and then centrifugation was conducted. This procedure was repeated until the test of chloride ions using $AgNO_3$ showed negative. To test for chloride ions, one drop of 0.1 M $AgNO_3$ was added to the pooled supernatant to observe a white haze of AgCl. Once no noticeable AgCl haze was observed, 30 mL of deionized water was added to the glucan precipitate. The mixture was heated in a boiling water bath for 30 min and titrated using 0.01 M NaOH. The DS was calculated by

$$\mathrm{DS} = \frac{162A}{1000 - 210A} \quad (1)$$

where A (mmol/g) is the molar amount of octenyl succinate groups in one gram of derivative, and 162 and 210 are the molecular weights of the anhydro glucosyl unit and the octenyl succinate group, respectively. The value of A was calculated as

$$A = \frac{(V - V_0) \times 0.01}{0.5} \quad (2)$$

In eq 2, V (mL) is the volume of NaOH solution consumed by the octenyl succinate derivative, V_0 (mL) is the volume of NaOH consumed by native phytoglycogen or starch, 0.5 is the weight of material in grams and 0.01 is the molar concentration of NaOH.

Dispersed Molecular Density. Weight-average molecular weight (M_W), *z*-average radius of gyration (R_Z) of phytoglycogen, waxy corn starch, and their octenyl succinate derivatives were determined using an HPSEC-MALLS-RI system (Wyatt Technology, Santa Barbara, CA) using two connected columns (PL Aquagel-OH 40 and 60, Polymer Laboratories, Varian Inc.) with a guard column. The flow rate was

Table 1. Degree of Substitution (DS), Substitution Efficiency (SE), Weight-Average Molecular Weight (M_W), *z*-Average Radius of Gyration (R_Z), Dispersed Molecular Density (ρ), and Zeta-Potential of Phytoglycogen, Waxy Corn Starch, and Their Derivatives after Reacting with 3 and 9% of Octenyl Succinic Anhydride (OSA)

	OSA, % of glucan	DS × 100[a]	SE, %	M_W, g/mol × 10^{-7} [b]	R_Z, nm[b]	ρ, g/mol·nm^3 [b]	zeta-potential[a]
phytoglycogen	0 (native)			3.11 ± 0.09 a	30.5 ± 0.3 a	1095 ± 63 a	−3.1 ± 0.1
	3	1.46 ± 0.03	63	2.94 ± 0.06 a	30.5 ± 1.2 a	1036 ± 104 a	−14.9 ± 0.4
	9	4.75 ± 0.06	68	3.14 ± 0.06 a	33.7 ± 0.2 b	824 ± 21 b	−20.3 ± 0.9
waxy corn starch	0 (native)			2.79 ± 0.05 a	60.5 ± 2.5 a	127 ± 14 a	−4.2 ± 0.0
	3	1.52 ± 0.02	66	1.41 ± 0.35 b	63.5 ± 5.0 a	56 ± 13 b	−12.0 ± 0.6
	9	4.82 ± 0.06	69	1.43 ± 0.12 b	66.7 ± 0.7 a	48 ± 4 b	−17.9 ± 0.9

[a] Data are expressed as mean ± SD (n = 3). [b] Data are expressed as mean ± SD (n = 3). Significant differences within phytoglycogen group or waxy corn starch group are denoted by different letters ($p < 0.05$).

1.0 mL/min using deionized water (pH 6.8, containing 0.02% NaN_3) as the mobile phase. Astra software (Version 5.3.4.10, Wyatt Technology) was used to determine M_W and R_Z. The dispersed molecular density (ρ, g/mol·nm^3) was calculated as $\rho = M_W/R_Z^3$ (*6*). ANOVA was conducted using Minitab 15 (Minitab Inc., State College, PA), and the Tukey test was utilized with a significant F test ($P \leq 0.05$).

Emulsion Preparation. For phytoglycogen octenyl succinate (PG-OS) and waxy corn starch octenyl succinate (WCS-OS) materials, 1 g (dry base) of each was dispersed in 0.02 M NaAc buffer to make a 20 g dispersion. WCS-OS requires heating in a boiling water bath for 20 min for full dispersion. For Tween 20, 0.1 g was dissolved in buffer to make 20 g solution. For groups added with ε-polylysine (EPL), 77.6 μL of 25.8% EPL solution was added to the mixture. This made the concentration of EPL to be 0.10%. In addition, for the emulsions using PG-OS (prepared using 3% OSA) as the emulsifier, 38.8 and 155.2 μL of 25.8% EPL solution were added to the mixture, which made the EPL concentration to be 0.05 and 0.20%, respectively. For individual dispersions, the pH was adjusted to 6.0, and 0.50 g of fish oil was added. A coarse emulsion of fish oil was prepared using a high-speed mixer (T25 ULTRA-TURRAX, IKA) for 1 min at 18,000 rpm. The coarse emulsions were further treated using high pressure homogenizer (Nano DeBEE) at 34.5 MPa for two cycles.

The use of 5% PG-OS (or WCS-OS) and 0.5% of Tween 20 was based on the consideration to provide roughly the equivalent amount of hydrophobic moieties. For 1 g of PG-OS or WC-OS with DS around 0.015, around 0.09 mmol of hydrophobic groups was provided. In contrast, 0.1 g of Tween 20 provided around 0.08 mmol of hydrophobic groups. For PG-OS and WCS-OS, multiple hydrophobic groups were grafted on each individual glucan molecule; therefore, it is highly likely that only a fraction of all hydrophobic groups may get access to the oil−water interface.

Storage and Sampling. Immediately after homogenization, an aliquot from each emulsion was used for the analysis of initial particle size, hydroperoxide, and thiobarbituric acid reactive substances (TBARS). All initial measurements were conducted within 3 h after homogenization. Meanwhile, 8 mL of each emulsion was transferred into a 50 mL capped tube and placed upright still in a water circulator at 55 °C. To monitor the physical and oxidative stability, aliquots were taken after 1, 2, 3, 4, 5, and 6 days of storage.

Measurement of Lipid Hydroperoxide. From each emulsion sample, an aliquot of 0.3 mL was added to 1.5 mL of isooctane/2-propanol (3:1 v/v) mixture. The mixture was vortexed for 1 min before centrifugation for 2 min at 3200*g*. After a preliminary evaluation of hydroperoxide amount for each sample, a proper amount of aliquot of the organic phase was added to a methanol/butanol (2:1 v/v) mixture to make up 3.0 mL. To this mixture, 15 μL of ammonium thiocyanate solution (3.94 M) was added, followed by adding 15 μL of ferrous iron solution. The mixture was vortexed and incubated for 20 min before measuring the absorbance at 510 nm.

Ferrous iron solution was prepared by (1) dissolving 2 g of $FeSO_4 \cdot 7H_2O$ in 50 mL of deionized water, (2) dissolving 1.6 g of $BaCl_2$ dehydrate in 50 mL of water, (3) slowly mixing the solutions of $FeSO_4$ and $BaCl_2$, (4) adding 2 mL of 10 N HCl, and (5) collecting the clear solution of $FeCl_2$ after removing $BaSO_4$ precipitate. The ferrous iron solution was stored at 4 °C in the dark.

To prepare the ferric ion solution for the standard curve, 0.5 g of iron powder was dissolved in 50 mL of 10 M HCl, and 2 mL of a 30% H_2O_2 solution was added. The solution was heated in a boiling water bath for 5 min. After cooling, the solution was diluted with deionized water to 500 mL. The resulting ferric ion standard solution (1000 μg/mL) was further diluted with 1 M HCl to obtain final concentrations of 750, 500, 250, and 125 μg/mL.

Measurement of Thiobarbituric Acid Reactive Substances (TBARS). After a preliminary evaluation of TBARS for each sample, an aliquot of 0.4 mL of emulsion was added to 0.8 mL of thiobarbituric acid−butylated hydroxytoluene (TBA−BHT) solution. The mixture was vortexed for 30 s and heated in a boiling water bath for 15 min. Thereafter, the mixture was cooled to room temperature and centrifuged at 8500*g* for 10 min. The absorbance of supernatant was measured at 532 nm.

The TBA solution was prepared by mixing 15 g of trichoroacetic acid, 0.375 g of TBA, 1.76 mL of 12 M HCl and 82.9 mL of deionized water. The solution of 2% BHT was prepared by dissolving butylated hydroxytoluene in ethanol. TBA−BHT solution was prepared by slowly adding 3 mL of BHT solution into 100 mL of TBA solution with stirring.

Standard malonaldehyde (MDA) solution was prepared by dissolving 25 μL of 1,1,3,3 tetraethoxypropane (TEP) in 100 mL of water to make a 1.0 μmol/mL stock solution. Right before the test, 1.0 mL of stock solution was mixed with 50 mL of 1% (v/v) H_2SO_4 and then incubated for 2 h at room temperature. The resulting MDA standard was 20 nmol/mL. Series of dilutions using 1% H_2SO_4 were made to obtain 15, 10, and 5 nmol/mL standards (*25*).

Measurement of Emulsion Particle Size. The emulsions were diluted using 62.5 volumes of 0.01 M NaAc buffer pH 6.0. Thereafter, the particle size was measured at room temperature using a Zetasizer Nano (ZS90, Malvern Instruments).

Measurement of Zeta-Potential of Dispersions and Emulsions. To prepare dispersions containing PG-OS and EPL, PG-OS prepared using 3% OSA (with DS of 0.0146) was mixed with EPL in 0.02 M pH 6.0 NaAc buffer. For individual dispersions, the concentration of PG-OS was 5% (w/w), and EPL was 0.025, 0.05, 0.1, 0.2, and 0.4% (w/w). To prepare emulsions containing PG-OS and EPL, two procedures were conducted: (1) EPL added *before* emulsification and (2) EPL added *after* emulsification. The procedure of emulsification was described earlier. The amount of PG-OS was 5%, and the amount of EPL was 0.025, 0.05, 0.1, 0.2, and 0.4% for both groups with EPL added either before or after emulsification. In each emulsion, 2.5% (w/w based on buffer) of fish oil was used. To measure zeta-potential, dispersions and emulsions were diluted by 62.5 volumes of 0.01 M pH 6.0 NaAc buffer. The measurement was made using Zetasizer Nano at room temperature.

RESULTS AND DISCUSSION

Preparation of Phytoglycogen Octenyl Succinate (PG-OS) and Waxy Corn Starch Octenyl Succinate (WCS-OS). As shown in **Table 1**, the degree of substitution (DS) was slightly affected by the type of substrate: phytoglycogen (PG) or waxy corn starch (WCS). When the octenyl succinic anhydride (OSA) was used at 3% of glucan, the DS value was 0.0146 and 0.0152 for phytoglycogen octenyl succinate (PG-OS) and waxy corn starch octenyl succinate (WCS-OS), respectively. When OSA was added at 9%, the DS value was 0.0475 for PG-OS and 0.0482 for WCS-OS. The substitution efficiency (SE) for 9% OSA (68−69%) was slightly

higher than that for 3% OSA (63−66%). In general, the DS values were equivalent between PG-OS and WCS-OS at either the 3 or 9% OSA levels, which allowed direct comparisons between PG-OS and WCS-OS materials.

Molecular Weight, Radius of Gyration, Dispersed Molecular Density, and Zeta-Potential. The content of amylose in WCS is negligible due to the deficiency of granule-bond starch synthase (*2*). Therefore, the dispersion of WCS is a dispersion of amylopectin, a branched α-D-glucan (*7*). As shown in **Table 1**, the weight-average molecular weight (M_W) of PG (3.11×10^7 g/mol) was higher than that of WCS (2.79×10^7 g/mol). However, the *z*-average radius of gyration (R_Z) value of PG (30.5 nm) was much lower than that of WCS (60.5 nm), which resulted in a large difference of dispersed molecular density (ρ) in aqueous solution. The ρ value for PG was 1095 g/mol·nm^3, compared to 127 g/mol·nm^3 for WCS. Such a large difference in ρ was consistent with the result reported by Wong et al. (*6*).

Substitution with OS groups had no significant effect on the M_W of PG. Native PG had a M_W of 3.11×10^7 g/mol, the M_W for PG-OS with DS 0.0146 and 0.0475 were 2.94 and 3.14×10^7 g/mol, respectively. In contrast, OS substitution reduces the M_W of WCS. For native WCS, M_W was 2.79×10^7 g/mol. For WCS-OS with DS 0.0152 and 0.0482, M_W was reduced to 1.41 and 1.43×10^7 g/mol, respectively. The mechanism of molecular degradation associated with OS substitution of WCS is unknown. However, it is possible that the high pH value (8.5−9.0) encountered during reaction led to minor hydrolysis of glucosidic linkages. PG was more resistant to degradation than amylopectin, suggesting its higher structural integrity compared to amylopectin.

It appears that the OS substitution only slightly changed R_Z of PG and WCS (**Table 1**). At pH 6.8 (pH value of the mobile phase of HPSEC-MALLS-RI), OS groups were negatively charged, which resulted in repulsion among neighboring chain segments. The structural integrity of PG-OS restricts the stretching of outer chains and limits the expansion of the nanoparticles, as evidenced by an almost negligible change of R_Z at lower DS and minor R_Z increase at higher DS. For WCS-OS, the flexibility and stretching of individual chains retained the R_Z value even after a substantial decrease of M_W from WCS to WCS-OS.

OS substitution affected the dispersed molecular density (ρ) of glucan molecules (**Table 1**). The ρ value was reduced from 1095 g/mol·nm^3 for native PG to 1036 and 824 g/mol·nm^3 for PG-OS with DS 0.0146 and 0.0475, respectively. Apparently, an increased DS led to reduced density, which is attributed to the slightly increased R_Z. For WCS, the ρ value was substantially reduced from 127 g/mol·nm^3 for native WCS to 56 and 48 g/mol·nm^3 for WCS-OS with DS 0.0152 and 0.0482, respectively. Evidently, OS substitution increased the difference of molecular density between PG and WCS. The ρ ratio between PG and WCS was increased from 8.6 for native glucans to 18.5 and 17.2 for DS around 0.015 and 0.048, respectively.

Zeta-potential values of PG, WCS, PG-OS, and WCS-OS are shown in **Table 1**. Higher DS led to higher zeta-potential, suggesting that higher amount of OS groups resulted in higher surface charge density. At equivalent DS, the zeta-potential of PG-OS was slightly higher than that of WX-OS, which might be related to the difference of surface morphology or charge distribution. More studies remain to be conducted to address this issue.

Lipid Oxidation of Emulsions without ε-Polylysine. Hydroperoxide value reflects the formation of intermediate compounds of lipid oxidation. As shown in **Figure 3A**, the accumulation of lipid hydroperoxide was increased during storage regardless the use of emulsifiers. The highest values for individual emulsifiers were similar (600−700 mmol/kg oil) and were reached after the fourth

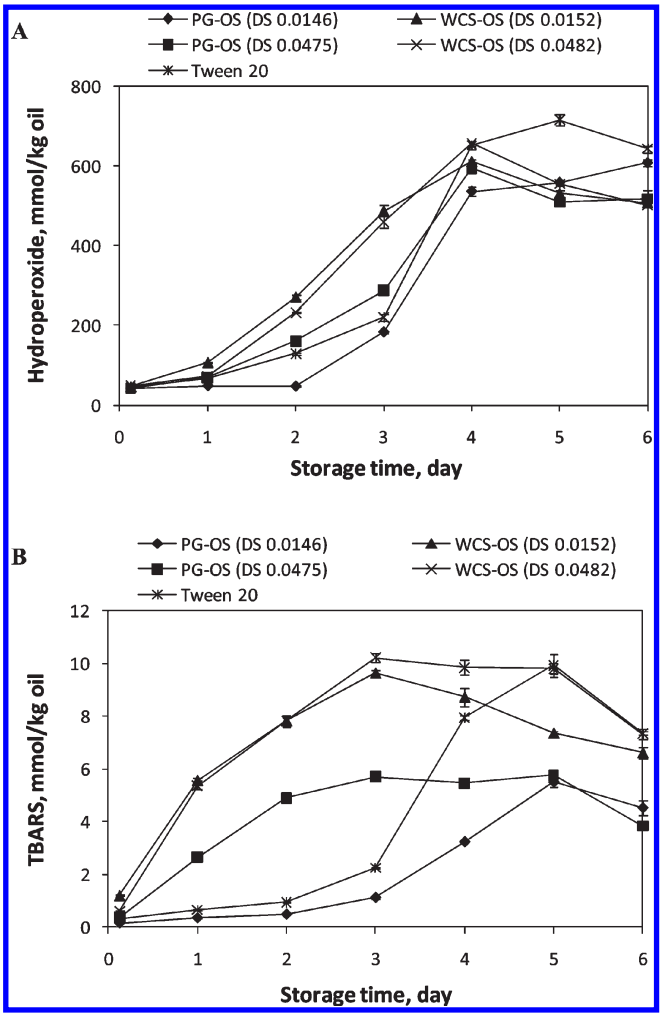

Figure 3. Accumulation of hydroperoxide (**A**) and TBARS (**B**) of fish oil emulsions formed by different types of emulsifier. Each data point is the mean value of 3 measurements with error bar of standard deviation.

day of storage at 55 °C. However, the initial hydroperoxide accumulation showed large differences among various emulsifiers, with the emulsion formed by PG-OS (DS 0.0146) having the lowest value before the fourth day, and in particular, before the second day. However, for the emulsion formed using PG-OS (DS 0.0475), hydroperoxide accumulation was much higher in the first 3 days, suggesting that an enhanced DS did not lead to reduced formation of hydroperoxide. Emulsions formed using WCS-OS had higher accumulation of hydroperoxide during the first four days than those using PG-OS. In addition, higher DS for WCS-OS led to slightly lower hydroperoxide at the early stages. In general, PG-OS materials were superior to WCS-OS in retarding the formation of hydroperoxide. Meanwhile, it is shown that the effect of Tween 20 ranged between those of two PG-OS materials and was inferior to PG-OS (DS 0.0146) all through the storage period.

The TBARS value reflects the formation of final products of lipid oxidation. As shown in **Figure 3B**, TBARS of the emulsion made with PG-OS (DS 0.0146) was much lower than that of other emulsifiers during the first 4 days of storage. At the fifth and sixth day, it approached and slightly surpassed the value of PG-OS (DS 0.0475). Similarly to hydroperoxide accumulation, PG-OS (DS 0.0475) was inferior to PG-OS (DS 0.0146) for controlling TBARS, and both PG-OS materials were much more effective than WCS-OS materials. The effect of Tween 20 on TBARS accumulation ranged between those of two PG-OS materials,

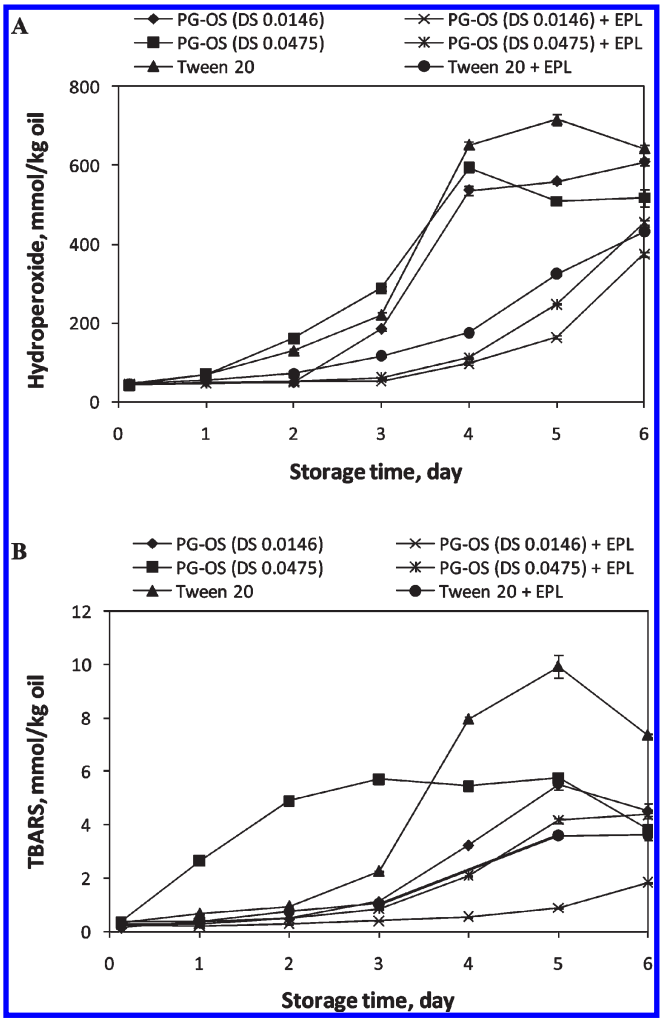

Figure 4. Accumulation of hydroperoxide (**A**) and TBARS (**B**) of fish oil emulsions formed using PG-OS and Tween 20, in the presence and absence of 0.1% ε-polylysine (EPL). Each data point is the mean value of 3 measurements with error bar of standard deviation.

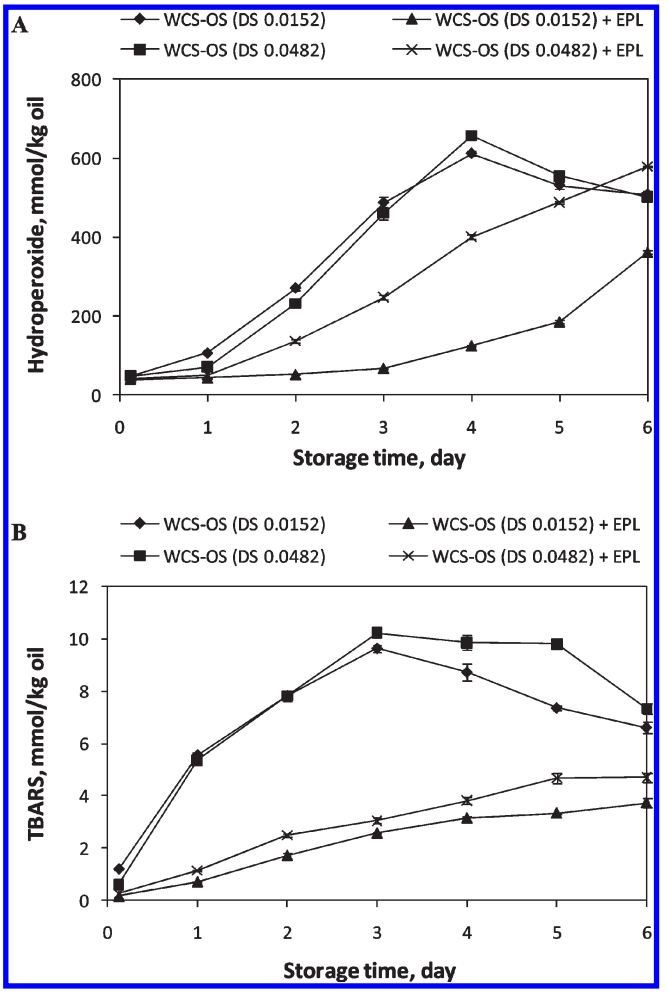

Figure 5. Accumulation of hydroperoxide (**A**) and TBARS (**B**) of fish oil emulsions formed using WCS-OS, in the presence and absence of 0.1% ε-polylysine (EPL). Each data point is the mean value of 3 measurements with error bar of standard deviation.

similar to the effect on hydroperoxide accumulation. Among all emulsifiers studied, PG-OS (DS 0.0146) showed the highest capability to retard the formation of both hydroperoxide and TBARS.

Lipid Oxidation of Emulsions with ε-Polylysine. Figures 4 and **5** compare the lipid oxidation in the presence or absence of 0.1% ε-polylysine (EPL). In general, the addition of EPL led to substantial reductions of both hydroperoxide and TBARS for all emulsions. For example, for PG-OS (DS 0.0146) emulsion the addition of EPL reduced the hydroperoxide from 536 to 96.3 mmol/kg oil at the fourth day, and from 608 to 374 mmol/kg oil at the sixth day (**Figure 4A**). Meanwhile, the TBARS was reduced from 3.2 to 0.6 mmol/kg oil at the fourth day, and from 4.5 to 1.8 mmol/kg oil at the sixth day (**Figure 4B**).

For emulsions without EPL, the accumulation of hydroperoxide usually reached the maximum before the sixth day. With EPL, the maximum before the sixth day was not seen for individual emulsions (**Figure 4A** and **Figure 5A**). Similarly, without EPL the accumulation of TBARS reached the maximum before the sixth day for all emulsions (**Figure 4B** and **Figure 5B**). In the presence of EPL, at the sixth day the maximum of TBARS was reached for emulsions of PG-OS (DS 0.0475), WCS-OS (DS 0.0482), and Tween 20, but not for PG-OS (0.0146) and WCS-OS (DS 0.0152) (**Figure 4B** and **Figure 5B**).

The effectiveness of EPL to reduce hydroperoxide and TBARS was different when it paired with different emulsifiers. This can be illustrated by comparing PG-OS (DS 0.0475) and Tween 20 at the third day. Due to the addition of EPL, hydroperoxide of PG-OS (DS 0.0475) was reduced by 227 mmol/kg oil (from 288 to 61 mmol/kg oil), which was much larger than the reduction of 104 mmol/kg oil for Tween 20 (from 220 to 116 mmol/kg oil) (**Figure 4A**). Similarly, at the third day, the addition of EPL led to a reduction of 4.9 mmol/kg oil of TBARS (from 5.7 to 0.8 mmol/kg oil) for PG-OS (DS 0.0475), much higher than the reduction of 1.2 mmol/kg oil (from 2.2 to 1.0 mmol/kg oil) for Tween 20 (**Figure 4B**). Conceivably, the antioxidative effect of EPL was associated with its interactions with emulsifiers.

The amount of EPL in emulsion had an appreciable effect on lipid oxidation. In **Figure 6**, comparisons were made among the use of 0.05, 0.1, and 0.2% of EPL, each paired with 5% PG-OS (DS 0.0146). In terms of reducing hydroperoxide, the effect of 0.05% EPL was slightly lower than that of 0.1% EPL. However, the use of 0.2% EPL led to hydroperoxide accumulation as high as that without EPL (**Figure 6A**). For TBARS accumulation, 0.2% EPL appeared to be more effective than 0.1% EPL, and TBARS of 0.05% EPL fall between those of 0.1% and no EPL (**Figure 6B**). It is considered that the high hydroperoxide accumulation for 0.2% EPL might be associated with low conversion of hydroperoxide to TBARS.

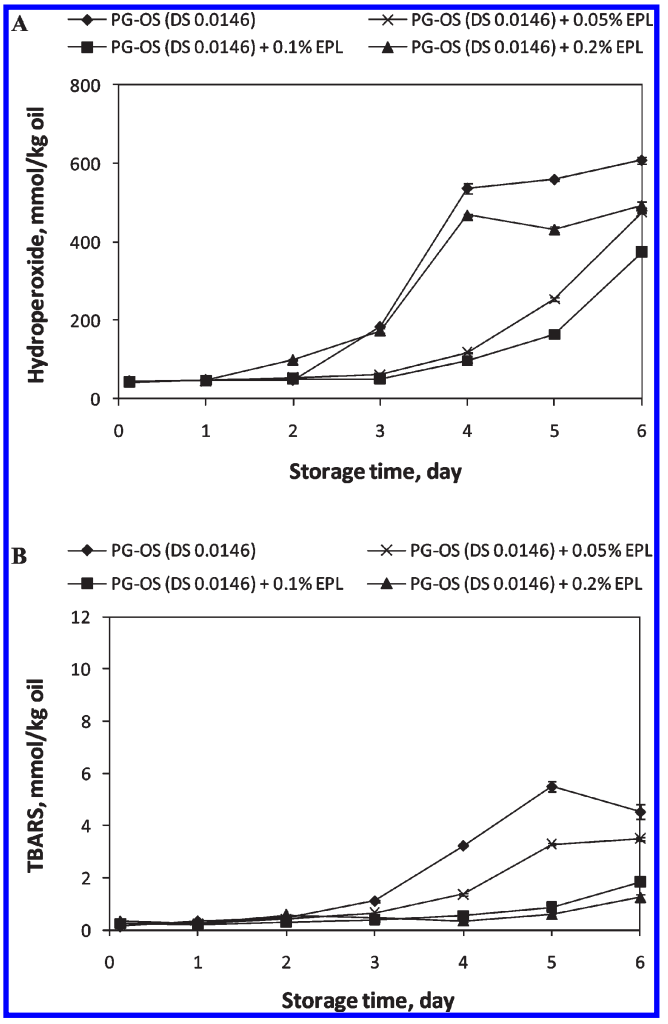

Figure 6. Accumulation of hydroperoxide (**A**) and TBARS (**B**) of fish oil emulsions formed using PG-OS (DS 0.0146), with ε-polylysine (EPL) added at 0.05, 0.1, and 0.2% levels. Each data point is the mean value of 3 measurements with error bar of standard deviation.

Particle Size of Emulsions during Storage. As shown in **Figure 7**, the particle size of emulsions was affected by emulsifiers. For example, the initial emulsion particle size of was 216, 303, 269, 393, and 507 nm for Tween 20, PG-OS (DS 0.0146), PG-OS (DS 0.0475), WCS-OS (DS-0.0152), and WCS (DS 0.0482), respectively. For PG-OS-stabilized oil droplets, the approximate thickness of the interfacial layer can be calculated using the R_Z of nanoparticles (**Table 1**). Therefore, the actual diameter of oil droplets stabilized using PG-OS (DS 0.0146) and PG-OS (DS 0.0475) should be around 181 nm (calculated from $303 - 30.5 \times 2 \times 2$ nm) and 134 nm (calculated from $269 - 33.7 \times 2 \times 2$ nm), respectively. These oil droplets should be smaller than those stabilized using Tween 20, since a layer of Tween 20 (molecular weight 1227 g/mol) should have very low contribution to the size of oil droplets (216 nm). In contrast, WCS-OS molecules would be more flexible than PG-OS due to its low molecular density; therefore it would be more difficult to evaluate the thickness of interfacial layer even though it might be in the scale of dozens of nanometers.

The physical stability of the emulsion was slightly different among individual emulsifiers (**Figure 7**). After 6 days of storage at 55 °C, the particle size was 209, 363, 314, 441, and 532 nm for Tween 20, PG-OS (DS 0.0146), PG-OS (DS 0.0475), WCS-OS (DS-0.0152), and WCS (DS 0.0482), respectively. Apparently, Tween 20 had the highest capability to maintain the particle

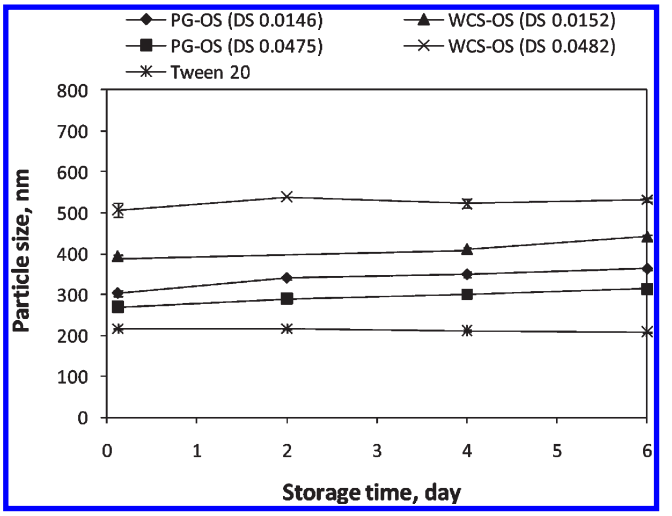

Figure 7. Average particle size of fish oil emulsions formed using PG-OS, WCS-OS, and Tween 20. Each data point is the mean value of 3 measurements with error bar of standard deviation.

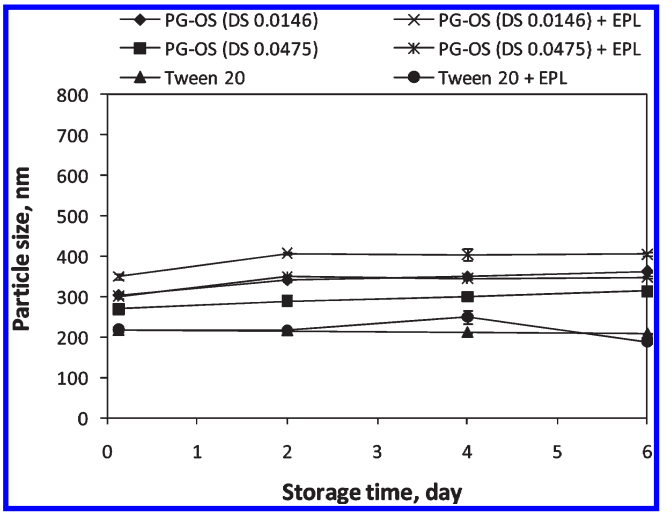

Figure 8. Average particle size of fish oil emulsions formed using PG-OS and Tween 20 in the presence and absence of 0.1% ε-polylysine (EPL). Each data point is the mean value of 3 measurements with error bar of standard deviation.

size of emulsion. Meanwhile, the increase of particle size was comparable among PG-OS and WCS-OS. In general, all the emulsions showed high physical stability during storage.

As shown in **Figure 8**, the addition of 0.1% EPL did not affect the physical stability of emulsions formed using Tween 20 and PG-OS. The reason for the fluctuation of particle size for Tween 20 emulsion remains unknown. Perhaps it was related to the interaction of EPL and Tween 20 at the interface. For both PG-OS emulsifiers, the presence of EPL increased the initial particle size by about 30−50 nm, which was retained all through the storage.

However, for emulsions made using WCS-OS, the addition of EPL led to a substantial increase of particle size during the 6-day storage (**Figure 9**). The particle size increased from 422 to 697 nm for WCS-OS (DS 0.0152) and from 399 to 568 nm for WCS-OS (DS 0.0482). Evidently, the physical stability of emulsions containing EPL was strongly affected by the structural differences between PG-OS and WCS-OS.

Zeta-Potential of Systems Containing Phytoglycogen Octenyl Succinate and ε-Polylysine. Zeta-potential is the electric potential between the slipping plane (within the interfacial double layer)

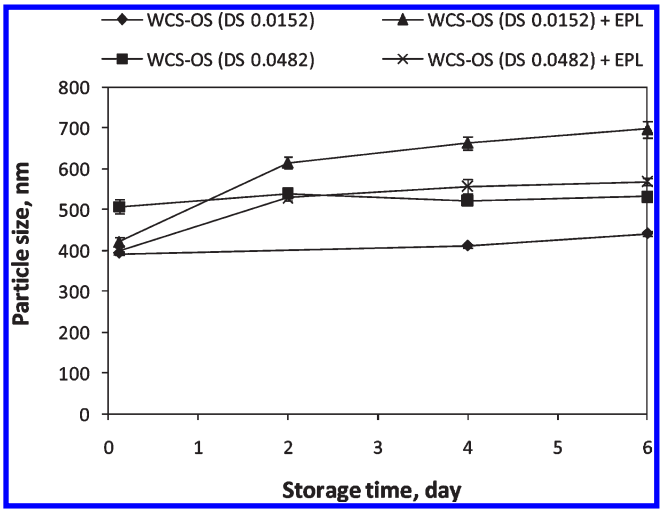

Figure 9. Average particle size of fish oil emulsions formed using WCS-OS in the presence and absence of 0.1% ε-polylysine (EPL). Each data point is the mean value of 3 measurements with error bar of standard deviation.

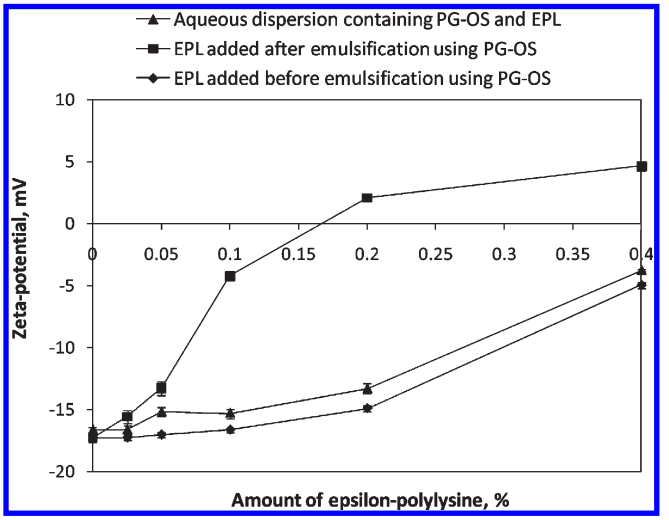

Figure 10. Zeta-potential of aqueous dispersions and emulsions containing both PG-OS (DS 0.0146) and ε-polylysine (EPL). Each data point is the mean value of 3 measurements with error bar of standard deviation.

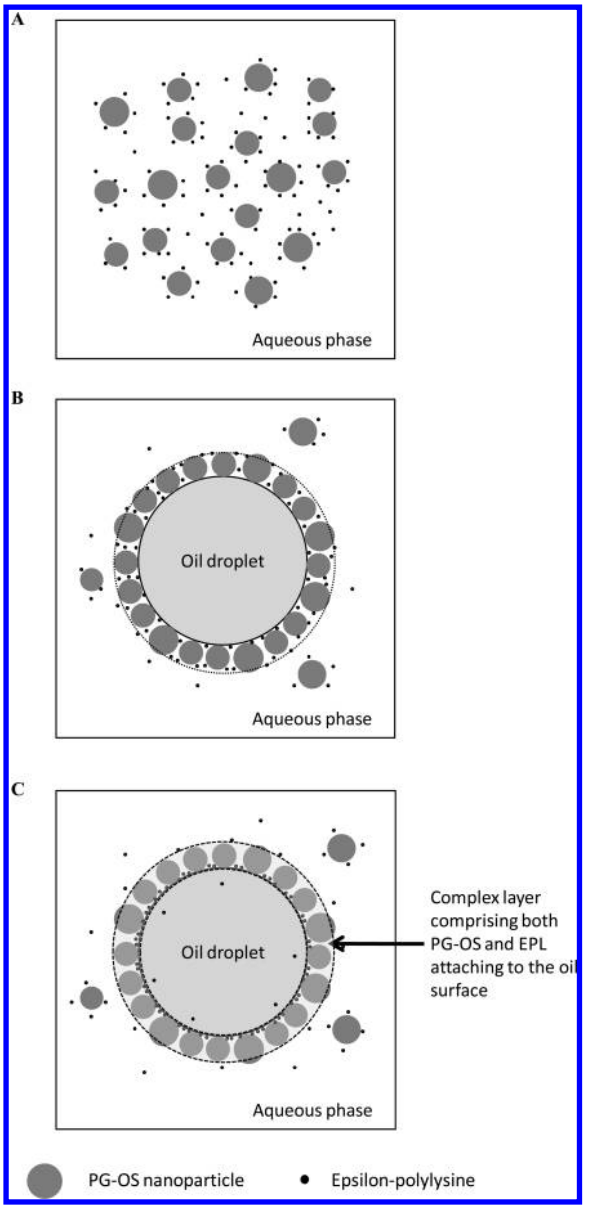

Figure 11. Schematic of distributions of PG-OS and ε-polylysine (EPL) in aqueous dispersion (**A**), emulsion with EPL added *after* emulsification (**B**), and emulsion with EPL added *before* emulsification (**C**). The label of PG-OS nanoparticle and EPL are indicated at the bottom. The complex layer comprising both PG-OS nanoparticles and EPL molecules is highlighted by the outer ring area (**C**).

and the bulk fluid away from the interface. It is a very useful parameter for evaluating the stability of colloidal dispersion and the interactions among charged molecules. In this study, zeta-potential was used to understand the interactions between EPL molecules and PG-OS nanoparticles in emulsions and aqueous dispersions.

Figure 10 shows the zeta-potential of systems containing 5% PG-OS and 0, 0.025, 0.05, 0.1, 0.2, and 0.4% EPL for (1) aqueous dispersions, (2) emulsions with EPL added *before* emulsification, and (3) emulsions with EPL added *after* emulsification. For the aqueous dispersions, when EPL was increased from 0 to 0.2%, the zeta-potential of PG-OS slightly changed from −16.63 mV to −13.30 mV. When EPL reached 0.4%, the zeta-potential changed to −3.77 mV. The result showed that, below 0.2%, the amount of EPL molecules at the slipping plane was not sufficient to cause a substantial change of zeta-potential. At a rather high content (0.4%), the partitioning of EPL molecules at the surface of nanoparticles increased, thus leading to a large reduction of zeta-potential. **Figure 11A** depicts the distribution of EPL in the PG-OS dispersion. In the schematic, there is an enrichment of EPL molecules in the vicinity of PG-OS nanoparticles; however, the portion of EPL molecules distributed at the slipping plane (shown as the boundary of particles) is rather low.

For the groups with EPL added *after* emulsification, the impact of EPL amount on zeta-potential was different from that for the aqueous dispersions. As shown in **Figure 10**, when EPL amount was increased from 0 to 2%, the zeta-potential was quickly changed from −17.23 mV to +2.10 mV, suggesting an effective neutralization of charged colloidal surface. **Figure 11B** depicts the distribution of EPL molecules in a PG-OS emulsion. At the oil−water interface, negatively charged PG-OS nanoparticles repel each other and form spaces among neighboring nanoparticles. EPL molecules added into PG-OS emulsion migrate toward the oil−water interface under two forces: (1) electrostatic interaction between positively charged EPL amino groups and negatively charged PG-OS carboxylate groups, and

(2) hydrophobicity of EPL molecules. At equilibrium (or possibly quasi-equilibrium), a portion of EPL molecules filled in the spaces formed by neighboring PG-OS nanoparticles. These EPL molecules could effectively neutralize the negative charge at the slipping plane of the PG-OS interfacial layer (indicated by the dotted circle). When EPL amount increases, the filling of EPL molecules effectively increases, causing rapid change of zeta-potential.

When EPL was added *before* emulsification, the increase of EPL resulted in a minor increase of the zeta-potential (**Figure 10**). When EPL increased from 0 to 0.2%, zeta-potential changed from −17.23 mV to −14.90 mV. When EPL reached 0.4%, zeta-potential was changed to −4.94 mV. This information is useful for evaluating the position of EPL molecules in emulsion. We believe that most EPL molecules were not in the bulk of the aqueous phase, since otherwise the system would be unstable and quickly transfer to the same state as that with EPL added *after* emulsification. It is highly possible that most EPL molecules were adsorbed at the oil surface, rather than at the outer surface of PG-OS interracial layer (**Figure 11C**). In this scenario, there could be a well-defined *complex layer* formed at the oil−water interface (**Figure 11C**). In the complex layer, both EPL molecules and PG-OS nanoparticles directly contact with oil phase. Due to the large size of PG-OS nanoparticles, the surface charge of entire droplet was governed by the negatively charged OS carboxylate groups.

Interfacial Complex Layer of Amphiphilic Nanoparticles and ε-Polylysine. EPL is amphiphilic, which allows for its interfacial enrichment even though it is a weak emulsifier (*26*). A stable EPL adsorption at the surface of oil droplets requires the formation of stable oil droplets and available adsorption sites. Stable oil droplets can be formed using regular emulsifiers; however, small-molecule emulsifiers (e.g., Tween 20) and structurally flexible polymeric emulsifiers (e.g., WCS-OS) may occupy a large portion of oil surface. In contrast, amphiphilic nanoparticles can be suitable emulsifiers to form stable oil droplets while providing available adsorption sites for EPL. The nanoparticles should be rigid enough to avoid excess coverage of adsorption sites by flexible chains.

Due to its structural integrity, PG-OS is a suitable material for forming stable oil droplets and providing adsorption sites for EPL. It is considered that the interfacial PG-OS/EPL complex layer has two basic functions: (1) being thick and dense, thus forming a strong physical barrier against for the permeation of pro-oxidative compounds (e.g., oxygen and metal ions) and (2) being positively charged at the surface of oil phase due to adsorbed EPL molecules, thus repelling metal ions. Therefore, a combined use of PG-OS and EPL effectively blocked the permeation of pro-oxidative compounds and resulted in high lipid oxidative stability of emulsions.

LITERATURE CITED

(1) James, M.; Robertson, D.; Myers, A. Characterization of the maize gene sugary1, a determinant of starch composition in kernels. *Plant Cell* **1995**, *7*, 417–429.

(2) Yao, Y. Biosynthesis of starch. In *Comprehensive Glycoscience*; Kamerling, H., Ed.; Elsevier: 2007.

(3) Myers, A.; Morell, M.; James, M.; Ball, S. Recent progress toward understanding the amylopectin crystal. *Plant Physiol.* **2000**, *122*, 989–997.

(4) Nakamura, Y. Towards a better understanding of the metabolic system for amylopectin biosynthesis in plants: Rice endosperm as a model tissue. *Plant Cell Physiol.* **2002**, *43*, 718–725.

(5) Putaux, J.; Buleon, A.; Borsali, R.; Chanzy, H. Ultrastructural aspects of phytoglycogen from cryo-transmission electron microscopy and quasi-elastic light scattering data. *Int. J. Biol. Macromol.* **1999**, *26*, 145–150.

(6) Wong, K.; Kubo, A.; Jane, J.; Harada, K.; Satoh, H.; Nakamura, Y. Structures and properties of amylopectin and phytoglycogen in the endosperm of sugary-1 mutants of rice. *J. Cereal Sci.* **2003**, *37*, 139–149.

(7) Thompson, D. B. On the non-random nature of amylopectin branching. *Carbohydr. Polym.* **2000**, *43*, 223–239.

(8) Shin, J.; Simsek, S.; Reuhs, B.; Yao, Y. Glucose release of water-soluble starch-related α-glucans by pancreatin and amyloglucosidase is affected by the abundance of α-1,6 glucosidic linkages. *J. Agric. Food Chem.* **2008**, *56*, 10879–10886.

(9) Caldwell, C. G.; Wurzburg, O. B. Polysaccharide derivatives of substituted dicarboxylic acids. United States Patent 2,661,349, 1953.

(10) Shogren, R. L.; Viswanathan, A.; Felker, F.; Gross, R. A. Distribution of octenyl succinate groups in octenyl succinic anhydride modified waxy maize starch. *Starch/Staerke* **2000**, *52*, 196–204.

(11) Bhosale, R.; Singhal, R. Effect of octenyl succinylation on physicochemical and functional properties of waxy maize and amaranth starches. *Carbohydr. Polym.* **2007**, *68*, 447–456.

(12) Song, X. Y.; He, G. Q.; Ruan, H.; Chen, Q. H. Preparation and properties of octenyl succinic anhydride modified early indica rice starch. *Starch/Staerke* **2006**, *58*, 109–117.

(13) Liu, Z. Q.; Li, Y.; Cui, F. J.; Ping, L. F.; Song, J. M.; Ravee, Y.; Jin, L. Q.; Xue, Y. P.; Xu, J. M.; Li, G.; Wang, Y. J.; Zheng, Y. G. Production of octenyl succinic anhydride-modified waxy corn starch and its characterization. *J. Agric. Food Chem.* **2008**, *56*, 11499–11506.

(14) Drusch, S.; Serfert, Y.; Scampicchio, M.; Schmidt-Hansberg, B.; Schwarz, K. Impact of physicochemical characteristics on the oxidative stability of fish oil microencapsulated by spray-drying. *J. Agric. Food Chem.* **2007**, *55*, 11044–11051.

(15) Shih, I. L.; Shen, M. H.; Van, Y. T. Microbial synthesis of poly (ε-lysine) and its various applications. *Bioresour. Technol.* **2006**, *97*, 1148–1159.

(16) Nawar, W. W. Lipids. In *Food chemistry*, 3rd ed.; Fennema, O. R., Ed.; Marcel Dekker: New York, 1996.

(17) Decker, E. A. Strategies for manipulating the pro-oxidative/antioxidative balance of foods to maximize oxidative stability. *Trends Food Sci. Technol.* **1998**, *9*, 241–248.

(18) McClements, D. J.; Decker, E. A. Lipid oxidation in oil-in-water emulsions: impact of molecular environment on chemical reactions in heterogeneous food systems. *J. Food Sci.* **2000**, *65*, 1270–1282.

(19) Ogawa, S.; Decker, E. A.; McClements, D. J. Influence of environmental conditions on the stability of oil in water emulsions containing droplets stabilized by lecithin-chitosan membranes. *J. Agric. Food Chem.* **2003**, *51*, 5522–5527.

(20) Klinkesorn, U.; Sophanodora, P.; Chinachoti, P.; Mcclements, D. J.; Decker, E. A. Increasing the oxidative stability of liquid and dried tuna oil-in-water emulsions with electrostatic layer-by-layer deposition technology. *J. Agric. Food Chem.* **2005**, *53*, 4561–4566.

(21) Guzey, D.; McClements, D. J. Formation, stability and properties of multilayer emulsions for application in the food industry. *Adv. Colloid Interface Sci.* **2006**, *128*, 227–248.

(22) Katsuda, M. S.; Mcclements, D. J.; Miglioranza, L. H. S.; Decker, E. A. Physical and oxidative stability of fish oil-in-water emulsions stabilized with beta-lactoglobulin and pectin. *J. Agric. Food Chem.* **2008**, *56*, 5926–5931.

(23) Kellerby, S. S; Gu, Y. S.; McClements, D. J.; Decker, E. A. Lipid oxidation in a menhaden oil-in-water emulsion stabilized by sodium caseinate cross-linked with transglutaminase. *J. Agric. Food Chem.* **2006**, *54*, 10222–10227.

(24) DS titration method CXAS. Joint FAO/WHO Expert Committee on Food Additives (JECFA) **1991**. Page 985.

(25) Pilz, J.; Meineke, I.; Gleiter, C. H. Measurement of free and bound malondialdehyde in plasma by high-performance liquid chromatography as the 2,4-dinitrophenylhydrazine derivative. *J. Chromatogr., B: Anal. Technol. Biomed. Life Sci.* **2000**, *742*, 315–325.

(26) Ho, Y.; Ishizaki, S.; Tanaka, M. Improving emulsifying activity of e-polylysine by conjugation with dextran through the Maillard reaction. *Food Chem.* **2000**, *68*, 449–455.

Received for review September 8, 2009. Revised manuscript received November 4, 2009. Accepted November 05, 2009.